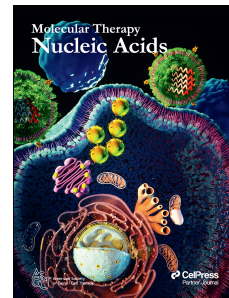


Journal Pre-proof

mRNA-1273 is placenta-permeable and immunogenic in the fetus

Jeng-Chang Chen, Mei-Hua Hsu, Rei-Lin Kuo, Li-Ting Wang, Ming-Ling Kuo, Li-Yun Tseng, Hsueh-Ling Chang, Cheng-Hsun Chiu



PII: S2162-2531(25)00043-5

DOI: <https://doi.org/10.1016/j.omtn.2025.102489>

Reference: OMTN 102489

To appear in: *Molecular Therapy: Nucleic Acid*

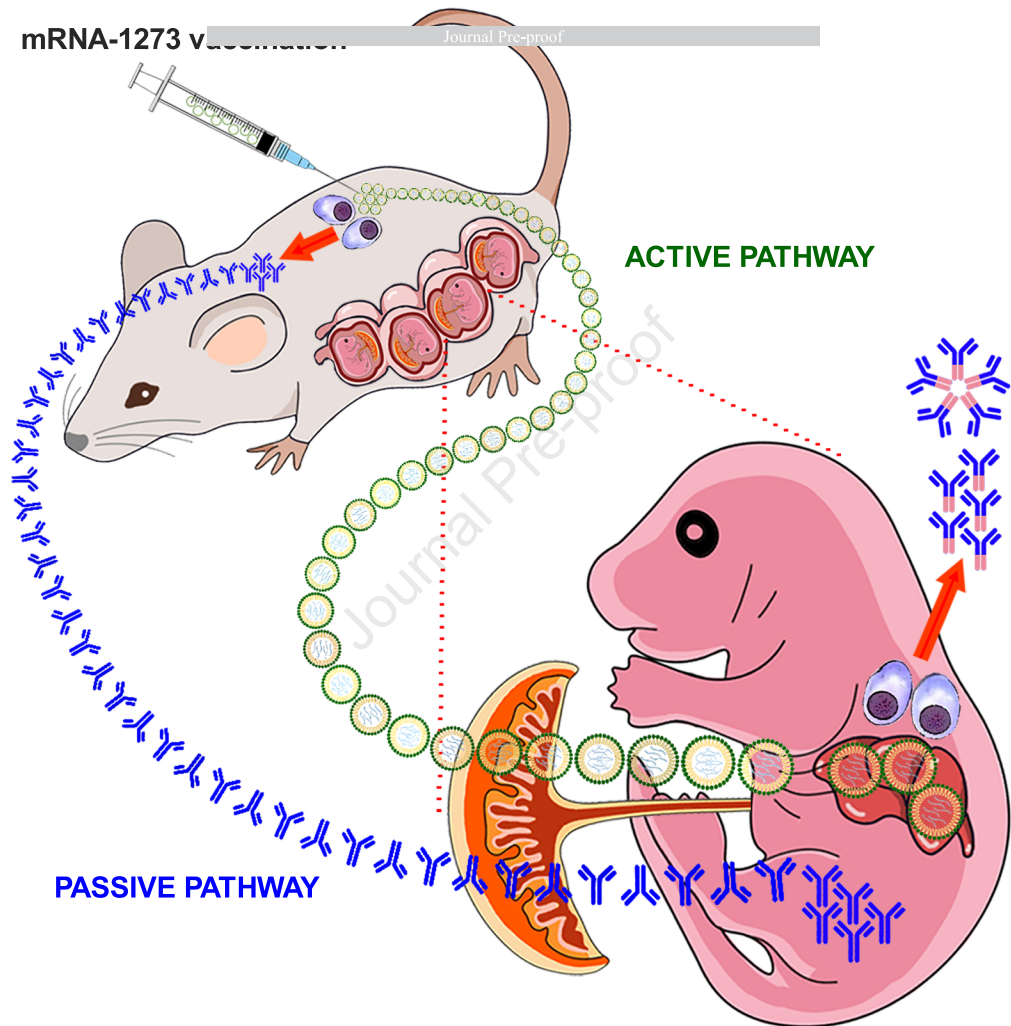
Received Date: 6 September 2024

Accepted Date: 13 February 2025

Please cite this article as: Chen J-C, Hsu M-H, Kuo R-L, Wang L-T, Kuo M-L, Tseng L-Y, Chang H-L, Chiu C-H, mRNA-1273 is placenta-permeable and immunogenic in the fetus, *Molecular Therapy: Nucleic Acid* (2025), doi: <https://doi.org/10.1016/j.omtn.2025.102489>.

This is a PDF file of an article that has undergone enhancements after acceptance, such as the addition of a cover page and metadata, and formatting for readability, but it is not yet the definitive version of record. This version will undergo additional copyediting, typesetting and review before it is published in its final form, but we are providing this version to give early visibility of the article. Please note that, during the production process, errors may be discovered which could affect the content, and all legal disclaimers that apply to the journal pertain.

© 2025 The Author(s). Published by Elsevier Inc. on behalf of The American Society of Gene and Cell Therapy.



ACTIVE PATHWAY

PASSIVE PATHWAY

1 **mRNA-1273 is placenta-permeable and immunogenic in the fetus**

2 **AUTHORS**

3 Jeng-Chang Chen^{1,2}, Mei-Hua Hsu^{3,4}, Rei-Lin Kuo^{5,6,7}, Li-Ting Wang⁶, Ming-Ling Kuo^{7,8}, Li-
4 Yun Tseng⁹, Hsueh-Ling Chang⁹, Cheng-Hsun Chiu^{3,4}

5 **AFFILIATIONS**

6 ¹ School of Medicine, College of Medicine, Chang Gung University, Taoyuan 333, Taiwan.

7 ² Division of Pediatric Surgery, Department of Surgery, Chang Gung Memorial Hospital,
8 Taoyuan 333, Taiwan.

9 ³ Division of Pediatric Infectious Diseases, Department of Pediatrics, Chang Gung Memorial
10 Hospital, Taoyuan 333, Taiwan

11 ⁴ Molecular Infectious Disease Research Center, Chang Gung Memorial Hospital, Taoyuan
12 333, Taiwan

13 ⁵ Department of Medical Biotechnology and Laboratory Science, College of Medicine, Chang
14 Gung University, Taoyuan 333, Taiwan

15 ⁶ Research Center for Emerging Viral Infections, College of Medicine, Chang Gung
16 University, Taoyuan 333, Taiwan

17 ⁷ Division of Allergy, Asthma, and Rheumatology, Department of Pediatrics, Chang Gung
18 Memorial Hospital, Taoyuan 333, Taiwan

19 ⁸ Department of Microbiology and Immunology, Graduate Institute of Biomedical Sciences,
20 College of Medicine, Chang Gung University, Taoyuan, Taiwan

21 ⁹ Pediatric Research Center, Chang Gung Memorial Hospital, Taoyuan 333, Taiwan

22

23 **Short Title:** Transplacental mRNA-1273 transfer

24 **Correspondence and requests for materials should be addressed to Cheng-Hsun Chiu,**

25 Department of Pediatrics, Chang Gung Memorial Hospital, No. 5, Fu-Shin Street, Kweishan,

26 Taoyuan 333, Taiwan. Phone: +886-3-3281200; Email: chchiu@adm.cgmh.org.tw

27 **Abstract**

28 COVID-19 mRNA vaccines are generally recognized as safe for gestational
29 administration. However, their transplacental pharmacokinetics remains obscure. In this study,
30 mRNA-1273 intramuscularly given to pregnant mice rapidly circulated in maternal blood and
31 crossed the placenta within one hour to spread in fetal circulation. Although spike mRNA in
32 fetal circulation faded away within 4-6 hours, it could accumulate in fetal tissues, mainly the
33 liver and get translated into spike protein. Transplacental mRNA-1273 proved immunogenic in
34 the fetuses, as postnatally equipped with anti-spike IgM, paternal allotypic anti-spike IgG_{2a} and
35 heightened anti-spike cellular immunity. Gestationally administered, mRNA-1273 had a dose-
36 dependent effect on its transplacental transfer and immunogenicity in the fetuses, with higher
37 mRNA-1273 doses leading to increased transplacental mRNA-1273 passage and greater serum
38 titers of endogenous anti-spike IgM/IgG generated by the fetuses. Thus, gestationally maternal
39 mRNA-1273 vaccination might endow the newborns with not only passive but also active anti-
40 spike immunity. Our results pose new insights into transplacental capacity of mRNA vaccines
41 and their immunogenic potential in the fetuses, advancing our knowledge of mRNA medicine
42 to protect the unborns against pathogens in perinatal life and broaden our horizons of prenatal
43 mRNA molecular therapy.

44 **Introduction**

45 The two next-generation vaccines of Moderna mRNA-1273¹ and BioNTech BNT162b2,²
46 based on SARS-CoV-2 spike protein-encoding mRNA strands packaged in lipid nanoparticles
47 (LNPs),³ have been widely used during and after COVID-19 pandemic. They conferred over
48 90% efficacy against COVID-19 with a favorable safety profile in adults.^{1,2} However,
49 heightened pharmacovigilance pertaining to potential or unexpected embryotoxic/fetotoxic
50 effects of brand-new medical products administered during pregnancy precluded gravid women
51 from mRNA-LNP vaccination at the outset⁴ even though COVID-19 during pregnancy tended
52 to pose a higher risk for maternal or neonatal complications.⁵ Since accumulated clinical data
53 and observations supported the safety of mRNA vaccines for the mother and fetus,⁵ mRNA-
54 LNP vaccination prior to⁶ or during pregnancy⁷ has been highly recommended. However, the
55 pharmacokinetics of mRNA-LNPs in gravid females remains shrouded in clouds, especially as
56 to their transplacental capacity. Although LNPs were reported to enable in vivo vascular
57 endothelial growth factor mRNA delivery to the placenta accompanied by its vasodilation,⁸
58 neither vaccine mRNA nor mRNA-decoded spike protein could be detected in the placenta⁹
59 and cord blood¹⁰ sampled 2 days at least and mostly over weeks or even months after final
60 maternal BNT-162b2 or mRNA-1273 vaccination. It brought to the notion that the placenta
61 acted as the natural barrier to mRNA-LNPs, providing additional reassurance about the safety
62 of mRNA vaccines during pregnancy. However, it was reported that mRNA-LNPs were swiftly
63 cleared from circulation during the first 24 hours with the time required for 50% decrement of
64 mRNA-LNP concentration ($T_{1/2}$) in a range of 2.7-3.8 hours,¹¹ implicating that transplacental
65 mRNA-LNP transfer, if any, would most likely occur within 24 hours after maternal
66 vaccination. Moreover, mRNA-LNPs administered intravenously in fetal¹² or adult animals¹³
67 underwent rapid systemic spread with preferential LNP accumulation and peak mRNA
68 functionality in the liver within 4 hours followed by decreasing protein levels at 24 hours after

69 injection or translation ceasing on day 2. Taken together, it seemed premature to negate
70 transplacental mRNA-LNP transfer on the basis of undetectable vaccine mRNA or its products
71 in belatedly-collected fetal blood or placenta that was even not favorable to harboring mRNA-
72 LNPs or spike proteins. We conducted this murine study to reappraise the transplacental
73 capacity of mRNA-1273 and scrutinize its immunogenicity in the fetuses.

Journal Pre-proof

74 **Results**

75 *Detection of transplacental polyethylene glycol (PEG) lipid*

76 Following a single-dose intramuscular injection of 4 μ g mRNA-1273 into gestational
77 day 14 (GD14) pregnant mice, the fetuses were delivered and sacrificed at selected time points
78 to search fetal blood for transplacental LNPs, using anti-PEG antibodies. PEGylated LNPs
79 swiftly moved into maternal bloodstream and efficiently crossed placenta to spread in fetal
80 circulation within 30 minutes (**Figure 1A**). However, they faded away in maternal circulation
81 within 3-24 hours but lasted over time in fetal circulation for at least 7 days, indicating slower
82 PEG breakdown in the fetuses than the dams. Further enzyme-linked immunosorbent assay
83 (ELISA) confirmed that PEG levels stayed steady in fetal sera within 3 hours after maternal 4
84 μ g mRNA-1273 vaccination, and dropped significantly at 6 hour and 1-3 day time points
85 (**Figure 1B**). PEG in offspring's sera was barely found on days 7-11 post-maternal vaccination,
86 and no longer detectable by days 14-18. There was no detectable PEG in fetal placenta, liver
87 and soft tissues by ELISA at any of the time points examined (data not shown). Notably, a
88 reduction of maternal mRNA-1273 doses caused a decline in serum PEG levels in the fetuses
89 within 3 hours after maternal vaccination (**Figure 1C**).

90 *Detection of transplacental spike mRNA*

91 We then examined whether transplacental LNP transfer was coupled with vaccine active
92 substance of SARS-CoV-2 spike mRNA by real-time polymerase chain reaction (RT-PCR)
93 (**Figure S1**). After maternal intramuscular vaccination of 4 μ g mRNA-1273, spike mRNA
94 entered maternal circulation and crossed the placenta to fetal blood within one hour, whereas
95 transplacental spike mRNA shortly became undetectable in fetal circulation by 4-6 hours
96 (**Table S1**). Thus, spike mRNA was more liable to degradation than PEG in fetal blood.
97 Transplacental spike mRNA mainly accumulated in fetal livers, and also dwelt in fetal placentas
98 and trunk soft tissues (**Figure 1D and Table S1**). Spike mRNA might persist in offspring's

99 liver and spleen at least till postnatal 3 weeks (**Table S1**). Notably, immunofluorescence
100 staining demonstrated the lodging of PEGylated LNPs and spike protein in fetal liver cells
101 (**Figure 1E**). Taken together, transplacental mRNA-1273 transfer came along with mRNA-
102 decoded protein expression in the fetus. In dams vaccinated with 0.2 μg mRNA-1273, vaccine
103 mRNA also rapidly spread to maternal circulation, accrued to the placenta and distributed to
104 the fetus (**Table S2**). Although levels of spike mRNA in fetal placentas did not differ between
105 0.2 and 4.0 μg mRNA-1273 administered to the dams, low-dose mRNA-1273 gave rise to less
106 spike mRNA accumulation in fetal livers than high-dose one (**Figure 1F**). Overall,
107 transplacental mRNA-1273 transfer exhibited a maternally dose-dependent response, with
108 higher maternal mRNA-1273 doses resulting in greater levels of PEG in the circulation and
109 spike mRNA in the liver of the fetus. However, comparable levels of spike mRNA in fetal
110 placentas between high and low-dose mRNA-1273 given to the dams might suggest placental
111 trapping of mRNA-1273 before reaching the fetus.

112 *Examination of anti-spike IgG₁/IgG_{2a} with their virus-blocking efficacy*

113 To elucidate the immunological consequences of transplacental mRNA-1273 transfer
114 in the fetus, we scrutinize the influence of mRNA-1273 doses given intramuscularly to pregnant
115 mice on serum anti-spike immunoglobulin levels of dams and pups. After maternal mRNA-
116 1273 vaccination at the same dose of 0.2, 1.0, 2.0 or 4.0 μg on GD14 and GD17, the dams and
117 their pups were examined for serum anti-spike immunoglobulin levels 1 month after delivery.
118 The vaccinated mothers significantly generated anti-spike IgG₁/IgG_{2a} in the absence of a dose-
119 responsive fashion, ranging respectively around 100-200 ng/mL and 20-40 $\mu\text{g}/\text{mL}$ with
120 relatively steady levels over a postnatal period of 3 months (**Figure 2A**). However, mRNA-
121 1273 given to pregnant mice exerted a dose-dependent effect on offspring's serum anti-spike
122 IgG₁/IgG_{2a} levels, which showed a dwindling trend over time (**Figure 2B**). Virus-blocking
123 efficacy of maternal sera was as high as 1024-2048-fold dilutions at least within postnatal 2-

124 3.5 months, whereas the pup's sera at 2 months old had lower neutralization activity, which
125 even vanished by 3.5 months old (**Figure 2C**). It was essentially consistent with the distinct
126 durability of serum anti-spike IgG between the dams (**Figure 2A**) and their offspring (**Figure**
127 **2B**). The discordance between the first month anti-spike IgG₁/IgG_{2a} levels of mothers and their
128 offspring in response to mRNA-1273 doses used to vaccinate the dams might have relevance
129 to transplacental mRNA-1273 transfer in a maternally dose-dependent manner (**Figures 1C&F**
130 **& Tables S1-2**). It called into question whether transplacental mRNA-1273 transfer was not
131 only maternally dose-dependent but also exerted a dose-dependent effect on triggering fetal
132 immune system to generate endogenous anti-spike IgG.

133 *Analyses of anti-spike IgG_{2a} allotypes in offspring*

134 Investigations proceeded to assess the derivation of offspring's anti-spike IgG_{2a} after
135 maternal mRNA-1273 vaccination, using two allelic forms (Igh-1a and Igh-1b) of the Igh-1
136 (IgG_{2a}, γ 2a constant region). The mouse BALB/c strain possesses the IgG_{2a} of Igh-1a haplotype,
137 whereas the C57BL/6 strain belongs to the Igh-1b haplotype. C57BL/6 females were mated to
138 BALB/c males, and then given 4 μ g mRNA-1273 vaccination respectively on GD14 and GD17.
139 Postnatally, the offspring (BALB/c male x C57BL/6 female, F1) co-expressed both Igh-1a and
140 Igh-1b haplotypes of anti-spike IgG_{2a} at their age of 4 weeks despite fading-out of Igh-1a
141 haplotype by 8 weeks old (**Figures 3A&B and Table S3**). It provided the direct molecular
142 evidence that the offspring were equipped with endogenous anti-spike IgG_{2a}, which could not
143 originate from anything other than offspring's B-cell clones selectively expressing paternal Igh-
144 1 allotype. Clearly, the offspring born to dams with gestational mRNA-1273 vaccination had
145 been immunized by spike protein and additionally armed with endogenous anti-spike IgG.
146 Incidentally, serum anti-spike IgG_{2a} of all C57BL/6 dams, mated to BALB/c males, was found
147 to contain Igh-1a haplotype of fetal origin (**Table S3**), indicating a reverse direction of fetal-to-
148 maternal anti-spike IgG_{2a} transfer. Thus, transplacental IgG transfer could be bidirectional.

149 When gestational C57BL/6 dams were vaccinated with 0.2 μ g mRNA-1273 twice, their
150 offspring barely generated anti-spike IgG_{2a} of Igh-1a haplotype despite high titers of Igh-1b
151 allotypic anti-spike IgG_{2a} in sera (**Figure 3C and Table S4**). These results pointed to a dose-
152 responsive relationship between mRNA-1273 doses used to vaccinate the dams and serum titers
153 of endogenous anti-spike IgG in the fetuses. As a consequence, mRNA-1273 had a maternally
154 dose-dependent effect on not only its transplacental capacity but also its immunogenicity as to
155 the productivity of endogenous anti-spike IgG in the fetuses.

156 *Assessment of anti-spike IgM and cellular immunity*

157 Being placenta-impermeable, anti-spike IgM in offspring was measured to reconfirm
158 fetal immunization by transplacental mRNA-1273. Maternal vaccination with either 0.2 or 4.0
159 μ g mRNA-1273 gave rise to heightened anti-spike IgM levels in offspring by their age of 4
160 weeks (**Figure 3D**). High-dose mRNA-1273 led to higher serum titers of fetal anti-spike IgM
161 than low-dose one. Vaccinated dams and their offspring were further examined for cellular
162 immunity to spike protein by the readout of incorporated tritium into lymphocytes. Both
163 compared favorably in spike protein-specific lymphocyte proliferation (**Figures 4A&B**) with
164 their respective saline control counterparts. Additionally, spike-reactive IFN- γ - and IL-2-
165 secreting T-cells were enumerated by Elispot, proving at significantly heightened frequencies
166 as opposed to their saline controls (**Figures 4C&D**). Altogether, maternal mRNA-1273
167 vaccination during pregnancy might trigger adaptive immunity against spike protein in dams
168 and their pups.

169 *Immunological outcome of direct fetal exposure to mRNA-1273*

170 To further validate the immunogenic effects of mRNA-1273 on pre-immune fetuses, we
171 directly subjected GD14 murine fetuses to intraperitoneal mRNA-1273 injection. Postnatally,
172 fetal recipients exhibited heightened titers of serum anti-spike IgG₁/IgG_{2a} (**Figures 5A&B**),
173 which decreased gradually within postnatal 3 months. Their lymphocytes also proliferated

174 specifically in response to SARS-CoV-2 spike protein (**Figure 5C**) in association with a
175 heightened frequency of spike-reactive IFN- γ and IL-2-secreting T-cells (**Figure 5D**). These
176 results signified fetal immunoreactivity to mRNA-1273 administered in utero even before full
177 T-cell development.

Journal Pre-proof

178 Discussion

179 Maternal mRNA COVID-19 vaccination during pregnancy offered a “two-for-one” deal
180 to protect mothers as well as their infants.⁷ This added infant protection has long since been
181 attributed to transplacental transfer of vaccine-elicited maternal anti-spike antibodies,^{4,7} likened
182 to maternal vaccination against influenza, tetanus, diphtheria and pertussis.¹⁴ In this study,
183 murine placentas proved permeable to mRNA-1273 along with mRNA-decoded spike protein
184 translation in GD14 murine fetuses, which lacked functionally competent T-cells as murine T-
185 cell receptors were not expressed until GD17.¹⁵ However, vertical mRNA-1273 transmission
186 made maternal mRNA-1273 vaccination immunogenic rather than tolerogenic in developing
187 fetuses. It’s in line with an immunization event arising after artificial fetal exposure to foreign
188 peptides,^{16,17} wherein fetal macrophages sequestered endocytosed antigens and differentiated
189 towards dendritic cells to instruct well-developed T-cells later on in life.¹⁶ Thus, developing
190 immune system of fetuses born to mothers with gestational mRNA-1273 vaccination still had
191 an active role in protecting against pathogens.

192 Mammalian placentas are categorized into epitheliochorial, endotheliochorial and
193 hemochorial types on the basis of the cell layers intervening between maternal and fetal
194 circulations,¹⁸ known as interhemal barriers that influence placental permeability of animal
195 species. Both humans and mice possess hemochorial placentas with similar cell types of
196 placental trophoblasts^{19,20} to mediate materno-fetal exchange. Hemochorial placentation lacks
197 interhemal barriers of uterine endometrium (including its epithelia, stroma and vascular
198 endothelia), leading to direct immersion of fetal trophoblast layers in maternal blood. It benefits
199 bio-substance exchange between mothers and their fetuses by providing direct access of fetal
200 trophoblasts to maternal blood.²¹ In light of the identical interhemal barriers in the placenta, the
201 mouse model should be appropriate for simulating placental exchange of bio-substances in
202 humans. However, one should exercise caution in extrapolating the findings of transplacental

203 mRNA-1273 transmission from this murine study to human subjects since there is a distinction
204 in histoarchitectures between murine and human placentas, evidenced by three-layered
205 trophoblasts (hemotrichorial) at murine materno-fetal interface in contrast to one-layered
206 syncytiotrophoblast (hemomonochorial) of human placenta.²⁰ It remained unclear whether the
207 two extra trophoblast layers in murine placentas exerted negative or positive impacts on
208 materno-fetal exchange of bio-substances, let alone mRNA-1273. This murine study
209 demonstrated that mRNA-1273 possessed the dose-dependent transplacental capacity in gravid
210 dams and exhibited immunogenic potential in the fetuses. These findings urge the need to
211 reappraise transplacental capacity of mRNA-LNPs and clarify the status of immunoreactivity
212 to spike protein in human fetuses or infants with gestational maternal mRNA COVID-19
213 vaccination. The information obtained will have a profound influence on the COVID-19
214 vaccination strategy in infants born to gestationally-vaccinated mothers.

215 mRNA vaccines exhibited good safety profiles in humans^{1,2} and even pregnant
216 individuals.²²⁻²⁴ However, the positive safety outcomes in the clinical arena could not alleviate
217 the apprehensions about the potential genotoxicity such as genome integration, oncogenesis or
218 germline transmission,²⁵⁻²⁷ which was fueled by enduring biodistribution of vaccine mRNA^{28,29}
219 or its product^{30,31} in post-marketing studies. These inconvenient findings somewhat reflected
220 the rapid marketing authorization of mRNA vaccines with incomplete preclinical studies due
221 to the urgent health needs in the face of a public health crisis caused by the COVID-19
222 pandemic.²⁵ This murine study filled the void in transplacental pharmacokinetics of mRNA
223 vaccines, which has been missing in preclinical studies even though mRNA vaccines
224 themselves involved several new biotechnologies. In this research, mRNA-1273 did not pose
225 discernible safety issues in pregnant mice and their pups. However, the proof of transplacental
226 mRNA-1273 transmission with enduring mRNA retention in offspring's liver or spleen
227 inevitably aroused an interest in the genotoxic effects of mRNA vaccines on the developing

228 fetus, where heightened activities of cell multiplication and specialization potentially created
229 genomic instability^{32,33} to render the fetus vulnerable to the integration of exogenous genetic
230 elements.^{34,35} Considering the occurrence of SARS-CoV-2 RNA retro-integration into human
231 cell genome,²⁶ the risk of long-term genotoxicity in the offspring born to mRNA-vaccinated
232 mothers cannot be overlooked.

233 Given the success of mRNA COVID-19 vaccines and today's biotech landscape, there is
234 a prospect of extending mRNA-LNP technology to the genetic diseases with defective/missing
235 proteins or enzymes such as cystic fibrosis, propionic acidemia, and phenylketonuria.³ These
236 candidate diseases if diagnosed prenatally can be managed by prenatal mRNA therapies before
237 the onset or in the early stage of irreversible pathology to minimize disease morbidity and
238 mortality, and achieve high therapeutic efficacy. In consideration of transplacental mRNA-
239 1273 passage, the unmet need of fetal mRNA therapies may be fulfilled simply through
240 maternal mRNA-LNP administration in case of no harm to the mothers, but the potential
241 immunogenicity of mRNA-decoded peptides must be taken into consideration even in pre-
242 immune fetuses. However, it's better to note that the ability of LNPs to deliver mRNA and
243 accumulate within desired tissues or organs varied with changes in LNP chemistry.^{12,36} Thus,
244 modifications in lipid excipients used for mRNA-LNP formulations might affect their
245 transplacental capacity and warrant an evaluation of their transplacental properties.

246 In this era of mRNA medicine, the new insights into transplacental pharmacokinetics of
247 mRNA vaccines and immunogenic potential of mRNA-decoded protein in the fetuses may
248 advance our knowledge to better protect the unborns against pathogens in perinatal life and
249 broaden our horizons of prenatal mRNA therapeutics.

250 **Methods**251 Mice

252 Inbred FVB/N, BALB/c (Igh-1a of IgG_{2a}, γ 2a constant region) and C57BL/6 (Igh-1b of
253 IgG_{2a}, γ 2a constant region) mice were purchased from National Laboratory Animal Center
254 (Taipei, Taiwan) at the age of 6-8 weeks. Animals were housed in Animal Care Facility at
255 Chang Gung Memorial Hospital (CGMH) under the standard guidelines from "Guide for the
256 Care and Use of Laboratory Animals" and with the approval of CGMH Committee on Animal
257 Research. Females were caged with males in the afternoon and checked for vaginal plugs the
258 following morning. The day of the plug observed was designated as day 0 of the pregnancy.

259 Harvest of fetal tissues

260 Under anesthesia for pregnant mice, midline laparotomy was performed to expose the uteri.
261 The fetuses were delivered through hysterotomy and immediately washed with saline. After
262 decapitation, fetal blood was collected by pipetmans. Then, fetal placenta, liver and trunk soft
263 tissues were obtained. Samples were stored in RNAlater solution at -80°C for downstream
264 analyses, or subjected to homogenization in organic solvents of ethanol or dimethyl sulfoxide
265 (DMSO) for PEG extraction.

266 mRNA-1273 vaccination in pregnant mice

267 Pregnant mice received intramuscular (thigh) injection of mRNA-1273 on their GD14 and
268 GD17, each at the same dose of 0.2, 1, 2 or 4 μ g, diluted in 100 μ l saline. Postnatally, sera of
269 the dams and their offspring were sampled periodically for downstream experimental analyses.
270 For mRNA-1273 component tracking in the fetuses, a single-dose of 0.2 or 4 μ g mRNA-1273
271 was intramuscularly given to the mothers on their GD14. The fetuses were then delivery by
272 Caesarean section at indicated time points after maternal vaccination to harvest fetal tissues and
273 placentas for downstream analyses.

274 In utero injection of mRNA-1273

275 Under anesthesia, the uteri of GD14 pregnant mice were exposed through a vertical
276 laparotomy. A 60 μm glass micropipette with beveled tip was used to inject 0.05-0.1 μg of
277 mRNA-1273 in 5 μl saline into the peritoneal cavities of all fetuses at a litter via trans-uterine
278 approach. The control mice received in utero saline injection. Murine abdomen was closed in
279 two layers by 5-0 silk suture. Then, mice were housed in an undisturbed room without bedding
280 changes for 1 week. Pups were weaned at 3 weeks of age.

281 Immunodot blot assay to detect LNPs of mRNA-1273

282 This method was modified from the fat blot assay by Munnik et al.³⁷ to semiquantitatively
283 detect mRNA-LNPs. Mouse sera and serially-diluted mRNA-1273 (1 μl for each sample) were
284 spotted onto a nitrocellulose membrane (0.45 NC, Amersham Protran). The membrane was first
285 blocked with 5% milk in Tri-buffered saline containing 0.05% Tween 20 (TBST) for 1 hour on
286 a rotating shaker and then incubated with anti-polyethylene glycol (PEG) antibody (1:3000,
287 PEG-B-47, ab51257, Abcam, reacting only with conjugated forms) for 2 hours. After TBST
288 washing for 3 times, the membrane was treated with peroxidase-conjugated goat anti-rabbit
289 IgG (1:5000, AP132P, Sigma-Aldrich) for 2 hours, followed by Immobilon Western
290 Chemiluminescent HRP Substrate (Millipore) for 2 minutes. Finally, the blots were subjected
291 to chemiluminescence imaging detection (UVP Chemstudio). Positive controls were 2-fold
292 serial dilutions of mRNA-1273, and negative controls included saline and maternal/pups' sera
293 collected after maternal saline injection.

294 Real-time quantitative polymerase chain reaction (RT-PCR) to detect spike mRNA^{10,38}

295 RNA was isolated from tissue samples of fetuses with maternal mRNA-1273 vaccination
296 using GeneJET RNA Purification Kit (Thermo Fisher Scientific) according to the
297 manufacturer's protocol. RNA concentration was determined using Nanodrop. RNA samples
298 of 500 ng were reversely transcribed into cDNA using PrimeScriptTM RT reagent Kit (TaKaRa
299 Bio). Primers used to detect target cDNA were as follows: Forward primer:

300 AACGCCACCAACGTGGTCATC. Reverse primer: GTTGTTGGCGCTGCTGTACAC. Bio-
301 Rad iQ5 real-time PCR detection system and 2xSYBR qPCR Mix (BioTools) were used for
302 PCR: 30s 95°C followed by 40 cycles of 5s 95°C and 20s 60°C. All samples (2 µL) were run
303 in duplicate as 20 µL reactions. For setup of spike mRNA standard curves, cDNA reversely-
304 transcribed from 100 ng/µL mRNA-1273 was serially diluted in 1:2 ratio. These 3-fold serial
305 dilutions of 2 µL cDNA samples were further 10x diluted to 20 µL (corresponding to 10⁴ -
306 0.0021 pg/µL of spike mRNA) in PCR amplification. Negative results were determined by the
307 Ct values of tissue samples from the fetuses with maternal saline injection.

308 Determination of serum anti-spike IgG₁, IgG_{2a} and IgM levels

309 ELISA microtiter plates (Corning, Corning, NY, USA) are first coated with 25 ng/ml and
310 50 ng/ml SARS-CoV-2 spike protein (GTX02774-pro, GeneTex) respectively for the
311 measurement of mouse anti-spike IgG₁ and IgG_{2a}/IgM levels. The wells are blocked with 3%
312 bovine serum albumin (BSA, Sigma-Aldrich) in PBS, and incubated with 100 µl of diluted
313 samples. In each well, biotinylated anti-mouse IgG₁ (Clone RMG1-1, BioLegend, San Diego,
314 CA, USA) was used for IgG₁ detection, biotinylated anti-mouse IgG_{2a} (Clone RMG2a-62,
315 BioLegend) for IgG_{2a} detection, and biotinylated anti-mouse IgM (Clone RMM-1, BioLegend)
316 for IgM detection. Subsequently, streptavidin-horseradish peroxidase (HRP, Sigma-Aldrich)
317 was added to the wells. Then, the reaction was developed by adding 100µl NeA-blue
318 tetramethylbenzidine substrate (TMB) (Clinical Science Products, Mansfield, MA, USA) and
319 stopped with 2M H₂SO₄. The optical density at 450 nm was read using an ELISA reader. Serum
320 anti-spike IgG₁ and IgG_{2a} levels were determined by the standard curves of mouse monoclonal
321 anti-SARS-CoV-2 spike IgG₁ (1A9, GTX632604, GeneTex) and mouse monoclonal anti-
322 SARS-CoV-1/2 S Protein IgG_{2a} (clone 2B3E5, Sigma-Aldrich), respectively. Serum anti-spike
323 IgM titers were recorded as the values of optical density.

324 Determination of anti-spike IgG_{2a} allotypes

325 Igh-1a and Igh-1b allotypes of IgG_{2a} were used to examine whether the pups (BALA/c
326 (Igh-1a) male x C57BL/6 (Igh-1b) female, F1) generated endogenous anti-spike IgG_{2a} after
327 maternal intramuscular vaccination of 0.2 or 4.0 µg mRNA-1273 respectively on GD14 and
328 GD17 during pregnancy. ELISA was performed as described above, using 10x diluted serum
329 samples treated with primary antibodies of biotinylated anti-mouse IgG_{2a} (1:20000, Clone
330 RMG2a-62, reacting with both Igh-1a and Igh-1b (Igh-1a/b) haplotypes), biotinylated anti-
331 mouse Igh-1a (1:2000, clone 8.3, BD Pharmingen) or biotinylated anti-mouse Igh-1b (1:2000,
332 clone 5.7, BD Pharmingen), respectively. The color developed was read at optic density of 450
333 nm. Controls included BALB/c (male) x BALB/c (female) and C57BL/6 (male) x C57BL/6
334 (female) F1 mice.

335 Quantification of PEG by sandwich ELISA

336 Sera or supernatants of tissue homogenates from murine fetuses were subjected to PEG
337 quantification by ELISA kits (Life Diagnostics, Cat. #: MPEG) with the capture antibody
338 specific to PEG backbone and the detection antibody to the terminal methoxy group of vaccine
339 PEGylated lipid. This sandwich ELISA was conducted according to the manufacturer's
340 instructions.

341 Lymphocyte proliferative responses to spike protein

342 Spleens were obtained from the mice (6-8 weeks old) with maternal mRNA-1273
343 vaccination during pregnancy. Splenic lymphocytes were enriched by density gradient
344 centrifugation and then cultured in triplicate each with 2×10^5 cells in 200 µL RPMI 1640
345 medium containing 10% fetal calf serum in 96-well plates. Responder lymphocytes were grown
346 in medium only as background controls, and stimulated with SARS-CoV-2 spike protein (1
347 µg/mL), third-party stimulator of BSA (100 ng/mL) or non-specific mitogen of Con-A (1
348 µg/mL). For the measurement of lymphocyte proliferation, day 5 cells were first subjected to
349 16-hour incubation with tritiated thymidine (ICN Biomedicals) at a final concentration of 1 µCi

350 per well and then harvested for counting incorporated tritium in a liquid scintillation counter
351 (1450 Microbeta Plus counter). Lymphocyte proliferation was determined by the readout of
352 incorporated tritium as counts per minute. Controls were the mice with maternal saline injection.

353 *IFN- γ and IL-2 enzyme-linked immunospot assay (ELISPOT)*

354 Murine IFN- γ /IL-2-secreting T-cells were quantified by mouse IFN- γ and IL-2 ELISpot
355 Kits according to the manufacturer's instructions (R&D Systems). Briefly, splenic lymphocytes
356 of each animal subject were enriched by density gradient centrifugation and then examined for
357 their CD3 T-cell fractions by flow cytometry after the treatment of fluorescence-conjugated
358 anti-CD3 antibodies (BioLegend). Wells in the microplates were first rinsed with culture media
359 of RPMI 1640 containing 10% fetal calf serum for 20 minutes at room temperature. Then, cells
360 were loaded into wells in triplicate at a dose of $10^6/100 \mu\text{l}$ culture media per well and incubated
361 in a humidified 37 °C CO₂ incubator for 2 days under the stimulation of SARS-CoV-2 spike
362 protein (1 $\mu\text{g/ml}$, GTX02774-pro, GeneTex). The plates were washed with Wash Buffer for 4
363 times and incubated with diluted Detection Antibody mixture (100 $\mu\text{l/well}$) for 2 hours at room
364 temperature on a rocking platform. After wash, the plates were incubated with diluted
365 Streptavidin-AP Concentrate A (100 $\mu\text{l/well}$) for 2 hours. The final wash was followed by the
366 treatment of BCIP/NBT Substrate for 1 hour. After the chromogen was decanted, the plates
367 were washed with deionized water and dried at room temperature. Plates were scanned and
368 counted on an immunospot analyzer (Cellular Technologies Ltd). The readouts of spike-
369 reactive IFN- γ /IL-2-secreting T-cells in each mouse were divided by its splenic CD3⁺ T-cell
370 fraction to estimate their frequencies per million T-cells.

371 *Neutralization assay with SARS-CoV-2 spike pseudovirus*³⁹

372
373 HEK-293T cells stably expressing human ACE2 (293T-ACE2 cells) were grown in 96-
374 well plates (6×10^4 cells/well) at 37°C with 5% CO₂ for 24 h. Serial 2-fold dilutions of mouse
375 sera were mixed with SARS-CoV-2 wild-type spike pseudotyped lentivirus containing

376 luciferase gene (4,000 relative infection unit), provided by RNA Technology Platform and
377 Gene Manipulation Core, Academia Sinica, in DMEM with 1% fetal bovine serum (FBS) at
378 37°C for 1 h. Then, the serum-pseudovirus mixtures were added to 293T-ACE2 cells, which
379 was incubated at 37°C with 5% CO₂ for 24 h and in DMEM with 10% FBS for another 24 h.
380 The luciferase activity was determined by Bright-Glo Luciferase Assay kit (Promega, Madison,
381 WI, USA) and the Synergy 2 (BioTek, Winooski, VT, USA) microplate reader. Neutralization
382 titer was determined by the highest serum dilution that reduced the viral infectivity by at least
383 50%, compared to the corresponding control wells without sera added.

384 *Histological examination of mRNA-LNPs and spike protein by immunofluorescence staining*

385 The fetuses was fixed in 4% paraformaldehyde overnight and embedded in paraffin. Tissue
386 sections were deparaffinized, rehydrated and then subjected to heat-induced antigen retrieval.
387 After permeabilized with Tween-20 and blocked with 1% BSA, the sections were incubated
388 with primary antibodies against PEG (1:100, PEG-B-47, ab51257, Abcam) and spike protein
389 (1:100, chimeric mAb, D001, MBS8119537) for 1.5 hr, followed by fluorescence-conjugated
390 donkey anti-rabbit IgG (1:100, Poly4064, BioLgend) and rat anti-human IgG Fc (1:100,
391 M1310G05, BioLgend). Visualization of the nuclei was achieved by Hoechst 33342 staining
392 (1: 20,000, Invitrogen). Sections were mounted with Dako fluorescence mounting medium.
393 Images were taken using a confocal microscope.

394 *Statistical Analyses*

395 All error bar charts were shown as 95% confidence intervals (boxed areas) for the means
396 (transverse lines crossing the boxes) along with superimposed data points of individual mice.
397 The equality of means was examined by Student's t-test between two independent or paired
398 groups, or by one-way analysis of variance (ANOVA) among three or more groups with post
399 hoc Fisher's least significant difference (LSD) multiple comparisons. Differences were
400 regarded as significant in all tests at $p < 0.05$.

401 **Keywords :** mRNA vaccine; lipid nanoparticle; transplacental transfer; maternal vaccination;
402 in utero immunization; IgG allotype

403

404 **Acknowledgments:** Special thanks go to Shiang-Chi Chen for her construction of graphic
405 abstract. Shiang-Chi Chen is now studying for Master of Fine Arts (MFA) in Visual
406 Development, Academy of Art University, San Francisco, California, USA.

407 This project was financially supported by NSTC-112-2314-B-182-033 (J.-C.C.) & NSTC-113-
408 2321-B-182-003 (C.-H.C.) from the National Science and Technology Council (NSTC),
409 Taiwan and CMRPG3N0931 (J.-C.C.) from Chang Gung Medical Foundation.

410

411 **Author contributions:** J.-C.C. conceptualized this study, acquired funding, performed in utero
412 injection, analyzed the data, prepared the figures and wrote the manuscript. M.-H.H. conducted
413 the experiments of all immunoassays and RT-PCR. R.-L.K. and L.-T.W. performed
414 pseudovirus neutralization assay. M.-L.K. helped to design the experiments of anti-spike IgG_{2a}
415 allotypes. L.-Y.T. and H.-L.C. performed immunostaining and assisted in experiments and
416 animal surgery as well as care. C.-H.C. conceptualized this study, acquired funding, assisted in
417 data analyses, supervised and coordinated the overall research and edited the manuscript.

418

419 **Declaration of interests:** The authors disclose no competing interests.

420

421 **Data and code availability**

422 Data reported in this paper will be shared by the correspondence author upon request.

423 Any additional information required to reanalyze the data reported in this paper is available
424 from the correspondence author upon request.

425 **References**

- 426 1. Baden, L.R., El Sahly, H.M., Essink, B., Kotloff, K., Frey, S., Novak, R., Diemert, D.,
427 Spector, S.A., Rouphael, N., Creech, C.B., et al. (2021). Efficacy and Safety of the
428 mRNA-1273 SARS-CoV-2 Vaccine. *N Engl J Med* 384, 403-416.
- 429 2. Polack, F.P., Thomas, S.J., Kitchin, N., Absalon, J., Gurtman, A., Lockhart, S., Perez,
430 J.L., Perez Marc, G., Moreira, E.D., Zerbini, C., et al. (2020). Safety and Efficacy of the
431 BNT162b2 mRNA Covid-19 Vaccine. *N Engl J Med* 383, 2603-2615.
- 432 3. Qin, S., Tang, X., Chen, Y., Chen, K., Fan, N., Xiao, W., Zheng, Q., Li, G., Teng, Y.,
433 Wu, M., et al. (2022). mRNA-based therapeutics: powerful and versatile tools to
434 combat diseases. *Signal Transduct Target Ther* 7, 166.
- 435 4. Gray, K.J., Bordt, E.A., Atyeo, C., Deriso, E., Akinwunmi, B., Young, N., Baez, A.M.,
436 Shook, L.L., Cvrk, D., James, K., et al. (2021). Coronavirus disease 2019 vaccine
437 response in pregnant and lactating women: a cohort study. *Am J Obstet Gynecol* 225,
438 303.e1-303.e17.
- 439 5. Jamieson, D.J., and Rasmussen, S.A. (2022). An update on COVID-19 and pregnancy.
440 *Am J Obstet Gynecol* 226, 177-186.
- 441 6. Halasa, N.B., Olson, S.M., Staat, M.A., Newhams, M.M., Price, A.M., Pannaraj, P.S.,
442 Boom, J.A., Sahni, L.C., Chiotos, K., Cameron, M.A., et al. (2022). Maternal
443 Vaccination and Risk of Hospitalization for Covid-19 among Infants. *N Engl J Med*
444 387, 109-119.
- 445 7. Rasmussen, S.A., and Jamieson, D.J. (2022). Covid-19 Vaccination during Pregnancy -
446 Two for the Price of One. *N Engl J Med* 387, 178-179.
- 447 8. Swingle, K.L., Safford, H.C., Geisler, H.C., Hamilton, A.G., Thatte, A.S., Billingsley,
448 M.M., Joseph, R.A., Mrksich, K., Padilla, M.S., Ghalsasi, A.A., et al. (2023). Ionizable

- 449 Lipid Nanoparticles for In Vivo mRNA Delivery to the Placenta during Pregnancy. *J*
450 *Am Chem Soc* *145*, 4691-4706.
- 451 9. Santos, A., Sauer, M., Neil, A.J., Solomon, I.H., Hornick, J.L., Roberts, D.J., Quade,
452 B.J., and Parra-Herran, C. (2022). Absence of SARS-CoV-2 Spike glycoprotein
453 expression in placentas from individuals after mRNA SARS-CoV-2 vaccination. *Mod*
454 *Pathol* *35*, 1175-1180.
- 455 10. Prahl, M., Golan, Y., Cassidy, A.G., Matsui, Y., Li, L., Alvarenga, B., Chen, H.,
456 Jigmeddagva, U., Lin, C.Y., Gonzalez, V.J., et al. (2022). Evaluation of transplacental
457 transfer of mRNA vaccine products and functional antibodies during pregnancy and
458 infancy. *Nat Commun* *13*, 4422.
- 459 11. (CHMP), C.f.M.P.f.H.U. (2021). Spikevax (previously COVID-19 Vaccine Moderna) :
460 EPAR - Public assessment report. European Medicines Agency, EMA/15689/2021.
- 461 12. Riley, R.S., Kashyap, M.V., Billingsley, M.M., White, B., Alameh, M.G., Bose, S.K.,
462 Zoltick, P.W., Li, H., Zhang, R., Cheng, A.Y., et al. (2021). Ionizable lipid
463 nanoparticles for in utero mRNA delivery. *Sci Adv* *7*, eaba1028.
- 464 13. Pardi, N., Tuyishime, S., Muramatsu, H., Kariko, K., Mui, B.L., Tam, Y.K., Madden,
465 T.D., Hope, M.J., and Weissman, D. (2015). Expression kinetics of nucleoside-modified
466 mRNA delivered in lipid nanoparticles to mice by various routes. *J Control Release*
467 *217*, 345-351.
- 468 14. Etti, M., Calvert, A., Galiza, E., Lim, S., Khalil, A., Le Doare, K., and Heath, P.T.
469 (2022). Maternal vaccination: a review of current evidence and recommendations. *Am J*
470 *Obstet Gynecol* *226*, 459-474.
- 471 15. Snodgrass, H.R., Kisielow, P., Kiefer, M., Steinmetz, M., and von Boehmer, H. (1985).
472 Ontogeny of the T-cell antigen receptor within the thymus. *Nature* *313*, 592-595.

- 473 16. Chen, J.C., Chan, C.C., Wu, C.J., Ou, L.S., Yu, H.Y., Chang, H.L., Tseng, L.Y., and
474 Kuo, M.L. (2016). Fetal Phagocytes Take up Allergens to Initiate T-Helper Cell Type 2
475 Immunity and Facilitate Allergic Airway Responses. *Am J Respir Crit Care Med* 194,
476 934-947.
- 477 17. Chen, J.C., Ou, L.S., Kuo, M.L., Tseng, L.Y., and Chang, H.L. (2020). Fetal exposure
478 to oncoantigen elicited antigen-specific adaptive immunity against tumorigenesis. *J*
479 *Immunother Cancer* 8, e000137.
- 480 18. Furukawa, S., Kuroda, Y., and Sugiyama, A. (2014). A comparison of the histological
481 structure of the placenta in experimental animals. *J Toxicol Pathol* 27, 11-18.
- 482 19. Malassine, A., Frendo, J.L., and Evain-Brion, D. (2003). A comparison of placental
483 development and endocrine functions between the human and mouse model. *Hum*
484 *Reprod Update* 9, 531-539.
- 485 20. Dilworth, M.R., and Sibley, C.P. (2013). Review: Transport across the placenta of mice
486 and women. *Placenta* 34 *Suppl*, S34-39.
- 487 21. Enders, A.C., and Carter, A.M. (2004). What can comparative studies of placental
488 structure tell us?--A review. *Placenta* 25 *Suppl A*, S3-9.
- 489 22. Shimabukuro, T.T., Kim, S.Y., Myers, T.R., Moro, P.L., Oduyebo, T.,
490 Panagiotakopoulos, L., Marquez, P.L., Olson, C.K., Liu, R., Chang, K.T., et al. (2021).
491 Preliminary Findings of mRNA Covid-19 Vaccine Safety in Pregnant Persons. *N Engl J*
492 *Med* 384, 2273-2282.
- 493 23. Zauche, L.H., Wallace, B., Smoots, A.N., Olson, C.K., Oduyebo, T., Kim, S.Y.,
494 Petersen, E.E., Ju, J., Beauregard, J., Wilcox, A.J., et al. (2021). Receipt of mRNA
495 Covid-19 Vaccines and Risk of Spontaneous Abortion. *N Engl J Med* 385, 1533-1535.
- 496 24. DeSilva, M., Haapala, J., Vazquez-Benitez, G., Vesco, K.K., Daley, M.F., Getahun, D.,
497 Zerbo, O., Naleway, A., Nelson, J.C., Williams, J.T.B., et al. (2022). Evaluation of

- 498 Acute Adverse Events after Covid-19 Vaccination during Pregnancy. *N Engl J Med*
499 387, 187-189.
- 500 25. Banoun, H. (2023). mRNA: Vaccine or Gene Therapy? The Safety Regulatory Issues.
501 *Int J Mol Sci* 24, 10514.
- 502 26. Zhang, L., Richards, A., Barrasa, M.I., Hughes, S.H., Young, R.A., and Jaenisch, R.
503 (2021). Reverse-transcribed SARS-CoV-2 RNA can integrate into the genome of
504 cultured human cells and can be expressed in patient-derived tissues. *Proc Natl Acad*
505 *Sci U S A* 118, e2105968118.
- 506 27. Guerriaud, M., and Kohli, E. (2022). RNA-based drugs and regulation: Toward a
507 necessary evolution of the definitions issued from the European union legislation. *Front*
508 *Med (Lausanne)* 9, 1012497.
- 509 28. Roltgen, K., Nielsen, S.C.A., Silva, O., Younes, S.F., Zaslavsky, M., Costales, C.,
510 Yang, F., Wirz, O.F., Solis, D., Hoh, R.A., et al. (2022). Immune imprinting, breadth of
511 variant recognition, and germinal center response in human SARS-CoV-2 infection and
512 vaccination. *Cell* 185, 1025-1040 e1014.
- 513 29. Fertig, T.E., Chitoiu, L., Marta, D.S., Ionescu, V.S., Cismasiu, V.B., Radu, E.,
514 Angheluta, G., Dobre, M., Serbanescu, A., Hinescu, M.E., et al. (2022). Vaccine mRNA
515 Can Be Detected in Blood at 15 Days Post-Vaccination. *Biomedicines* 10, 1538.
- 516 30. Ogata, A.F., Cheng, C.A., Desjardins, M., Senussi, Y., Sherman, A.C., Powell, M.,
517 Novack, L., Von, S., Li, X., Baden, L.R., et al. (2022). Circulating Severe Acute
518 Respiratory Syndrome Coronavirus 2 (SARS-CoV-2) Vaccine Antigen Detected in the
519 Plasma of mRNA-1273 Vaccine Recipients. *Clin Infect Dis* 74, 715-718.
- 520 31. Yonker, L.M., Swank, Z., Bartsch, Y.C., Burns, M.D., Kane, A., Boribong, B.P., Davis,
521 J.P., Loisele, M., Novak, T., Senussi, Y., et al. (2023). Circulating Spike Protein
522 Detected in Post-COVID-19 mRNA Vaccine Myocarditis. *Circulation* 147, 867-876.

- 523 32. Munisha, M., and Schimenti, J.C. (2021). Genome maintenance during embryogenesis.
524 DNA Repair (Amst) *106*, 103195.
- 525 33. Comaills, V., Kabeche, L., Morris, R., Buisson, R., Yu, M., Madden, M.W., LiCausi,
526 J.A., Boukhali, M., Tajima, K., Pan, S., et al. (2016). Genomic Instability Is Induced by
527 Persistent Proliferation of Cells Undergoing Epithelial-to-Mesenchymal Transition. *Cell*
528 *Rep* *17*, 2632-2647.
- 529 34. Mohrenweiser, H., and Zingg, B. (1995). Mosaicism: the embryo as a target for
530 induction of mutations leading to cancer and genetic disease. *Environ Mol Mutagen* *25*
531 *Suppl* *26*, 21-29.
- 532 35. Bose, S.K., Menon, P., and Peranteau, W.H. (2021). In Utero Gene Therapy: Progress
533 and Challenges. *Trends Mol Med* *27*, 728-730.
- 534 36. Trepotec, Z., Lichtenegger, E., Plank, C., Aneja, M.K., and Rudolph, C. (2019).
535 Delivery of mRNA Therapeutics for the Treatment of Hepatic Diseases. *Mol Ther* *27*,
536 794-802.
- 537 37. Munnik, T., and Wierchowicka, M. (2013). Lipid-binding analysis using a fat blot
538 assay. *Methods Mol Biol* *1009*, 253-259.
- 539 38. Golan, Y., Prahl, M., Cassidy, A., Lin, C.Y., Ahituv, N., Flaherman, V.J., and Gaw,
540 S.L. (2021). Evaluation of Messenger RNA From COVID-19 BTN162b2 and mRNA-
541 1273 Vaccines in Human Milk. *JAMA Pediatr* *175*, 1069-1071.
- 542 39. Liu, K.T., Gong, Y.N., Huang, C.G., Huang, P.N., Yu, K.Y., Lee, H.C., Lee, S.C.,
543 Chiang, H.J., Kung, Y.A., Lin, Y.T., et al. (2022). Quantifying Neutralizing Antibodies
544 in Patients with COVID-19 by a Two-Variable Generalized Additive Model. *mSphere*
545 *7*, e0088321.

546 **Figure Legends**547 **Figure 1. Transplacental mRNA-1273 transfer after maternal mRNA-1273 vaccination**548 **during pregnancy. (A)** GD14 FVB/N mothers, intramuscularly (IM) vaccinated with a single-

549 dose mRNA-1273 of 4.0 µg, were subjected to serum collection before vaccination (Pre), and

550 at indicated time points of 0.5-3 hours (h) and 1-7 days (d) after injection. Their pups were

551 delivered for serum sampling at the same time points. Immunodot blot assay demonstrated

552 transplacental PEGylated LNP transfer. **(B)** ELISA disclosed that fetal sera contained

553 significantly higher PEG levels at the time points of 1 h, 3 h, and 6 h after maternal mRNA-

554 1273 vaccination than those with maternal saline injection (Control, ANOVA with LSD

555 multiple comparison). A significant decrease of serum PEG levels occurred between 3 h and 6

556 h. Although PEG remained measurable in certain pups of groups 1-3 d and 7-11 d, their mean

557 levels did not differ from that of saline controls. On days 14-18, PEG was completely absent in

558 all neonatal sera, identical to saline controls. **(C)** At the time points of 1 h and 3 h following

559 maternal vaccination, 4.0 µg mRNA-1273 led to higher PEG levels in fetal sera than a dose of

560 0.2 µg. **(D)** Spike mRNA in fetal placenta, liver and soft tissue was quantified by RT-PCR after

561 maternal 4 µg mRNA-1273 vaccination (Dams 234, 235 and 236 in Table S1). Spike mRNA

562 levels of “(-)” and “< 0.021” were input as “0” and “0.021”, respectively in building this chart.

563 Spike mRNA significantly dominated in fetal liver of groups 1, 4 and 6 hr. (ANOVA with LSD

564 multiple comparison) **(E)** Immunostaining disclosed intracellular PEGylated LNPs and spike

565 protein in fetal liver 6 hours after maternal 4.0 µg mRNA-1273 vaccination. DIC: differential

566 interference contrast. ZI: zoom-in. **(F)** At the time points of 1, 4 and 6 hours after maternal

567 mRNA-1273 vaccination, levels of spike mRNA in fetal placentas did not differ between 4.0

568 and 0.2 µg mRNA-1273 used to vaccinate the dams (Tables S1-2), whereas 4.0 µg mRNA-1273

569 led to significantly greater spike mRNA accumulation in fetal livers than 0.2 µg mRNA-1273.

570

571 **Figure 2. Anti-spike IgG₁/IgG_{2a} with virus-blocking efficacy in dams and their offspring**
572 **after gestational mRNA-1273 administration.** Pregnant FVB/N mice were intramuscularly
573 vaccinated by the same doses of mRNA-1273 (0.2, 1, 2 or 4 µg) on GD14 and GD17. **(A)** One
574 month after delivery (M1), all the 4 mRNA-1273 doses elicited significant levels of serum anti-
575 spike IgG₁/IgG_{2a} in dams and **(B)** pups ($p < 0.001$, ANOVA), as compared with their saline
576 controls. There were dose-responsive anti-spike IgG₁/IgG_{2a} levels in pups rather than dams
577 (multiple comparisons by Fisher's LSD post hoc test). The dams (n=6) kept steady anti-spike
578 IgG₁/IgG_{2a} titers in sera within postnatal 3 months (M1-M3) except for an initial drop of anti-
579 spike IgG_{2a} levels ($p = 0.010$, pairwise comparison) at M2, whereas anti-spike IgG₁/IgG_{2a} in
580 pups' sera (n=18) gradually faded away by M3-M4. The interconnected circles at different time
581 points were the data of IgG₁/IgG_{2a} levels collected from an individual mouse. **(C)** Virus-
582 blocking efficacy of maternal and offspring's sera was evaluated by pseudovirus neutralization
583 assays, and shown in a representative mother and its offspring. Postnatal 2- and 3.5-month
584 maternal sera had the neutralization titers of 2048- and 1024-fold dilutions respectively,
585 whereas neutralization activity of offspring's sera was 64-fold at 2 months old but vanished by
586 3.5 months old.
587

588 **Figure 3. Analyses of anti-spike IgG_{2a} allotypes and anti-spike IgM in offspring born to**
589 **the dams with gestational mRNA-1273 vaccination. (A)** After mRNA-1273 vaccination,
590 BALB/c (Igh-1a) x C57BL/6 (Igh-1b) F1 mice (n=9) significantly secreted anti-spike IgG_{2a}
591 (Igh-1a/b) in sera within 2-4 weeks (pairwise comparison). Igh-1a haplotype dominated the
592 allotypes of anti-spike IgG_{2a}. **(B)** C57BL/6 females (F) mated to BALB/c males (M) were
593 vaccinated with 4 µg mRNA-1273 twice on GD14 and GD17. Both paternal Igh-1a and
594 maternal Igh-1b allotypic anti-spike IgG_{2a} significantly showed up in BALB/c (M) x C57BL/6
595 (F) F1 mice at 4 weeks old ($p < 0.001$) despite undetectable paternal Igh-1a allotype by 8 weeks
596 old ($p = 0.508$). **(C)** In the case of 0.2 µg mRNA-1273 vaccination in C57BL/6 pregnant mice,
597 BALB/c x C57BL/6 F1 offspring (n=17) did not compare favorably in serum anti-spike IgG_{2a}
598 of Igh-1a ($p = 0.418$) with their saline controls (n=5), but owned significantly higher levels of
599 Igh-1b ($p < 0.001$) allotype than the controls by their age of 4 weeks. **(D)** After maternal
600 vaccination with either 0.2 or 4.0 µg mRNA-1273 twice, offspring showed significantly
601 heightened levels of serum anti-spike IgM by their age of 4 weeks, as compared to the controls
602 with maternal saline injection. Besides, 4.0 µg mRNA-1273 given to the dams elicited higher
603 serum titers of anti-spike IgM in offspring than 0.2 µg mRNA-1273 ($p < 0.001$). OD: optic
604 density at 450 nm.

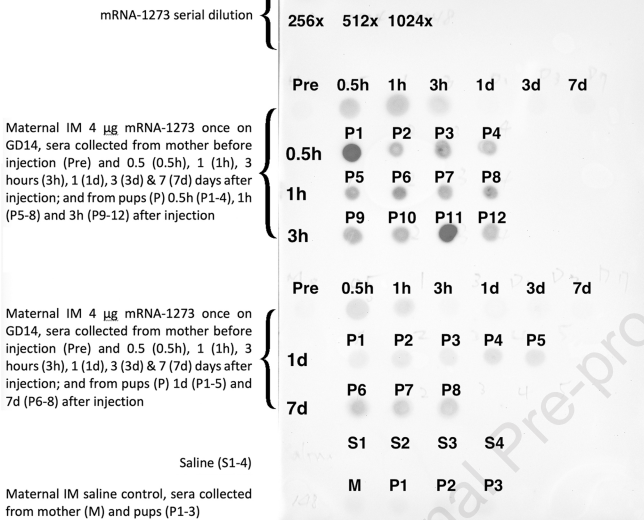
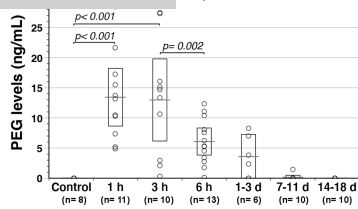
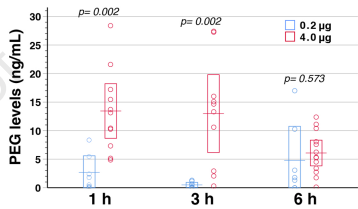
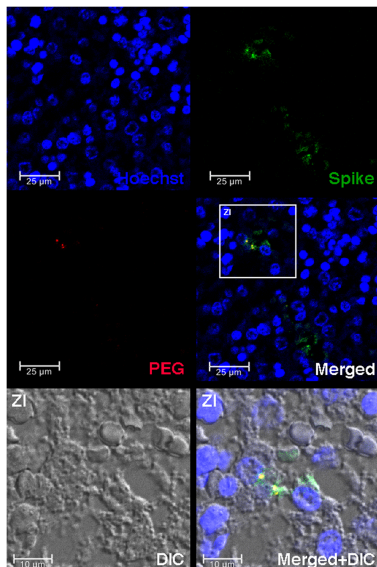
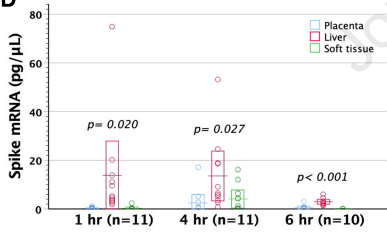
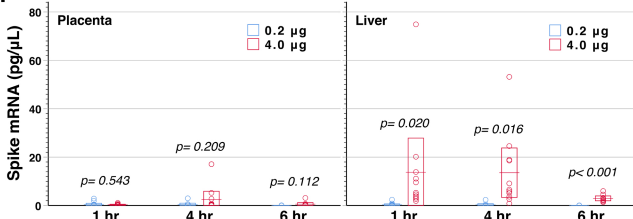
605

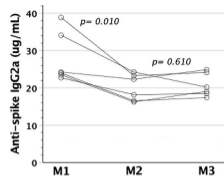
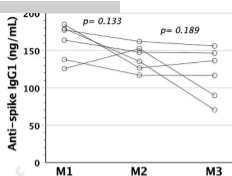
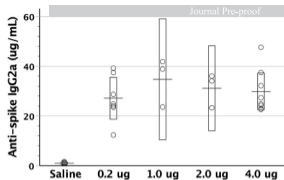
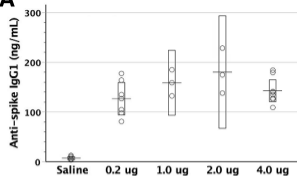
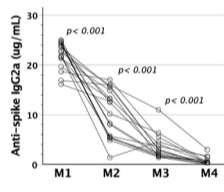
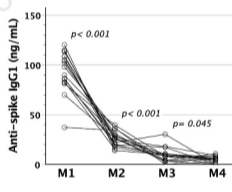
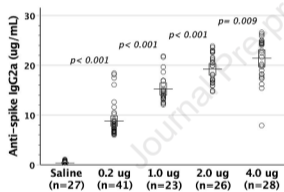
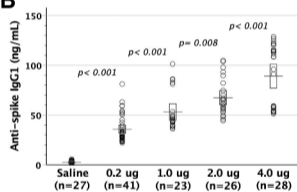
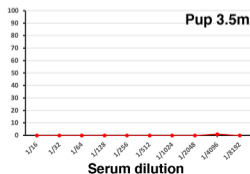
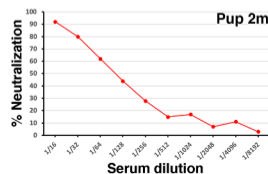
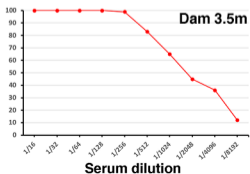
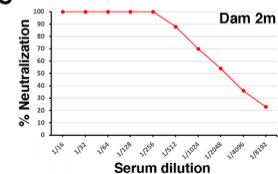
606 **Figure 4. Anti-spike cellular immunity in dams and their pups after maternal mRNA-**
607 **1273 vaccination during pregnancy. (A, B)** After maternal vaccination with 4 μ g mRNA-
608 1273 twice, the dams and pups were examined for spike-specific lymphocyte proliferation by
609 the readout of incorporated tritium in vitro. Splenic lymphocytes of both dams ($p= 0.001$) and
610 pups ($p< 0.001$) proliferated specifically in response to spike, as opposed to those with maternal
611 saline injection. Besides, the dams ($p= 0.004$) and pups ($p< 0.001$) with maternal mRNA-1273
612 vaccination were superior in spike-specific lymphocyte proliferation to their respective saline
613 controls. (C, D) IFN- γ - and IL-2 Elispot images in triplicate shown were from a representative
614 dam and pup with maternal mRNA-1273 (4 μ g) or saline vaccination during pregnancy. Both
615 groups exhibited heightened frequencies of IFN- γ - and IL-2-secreting T-cells, as compared
616 with their respective control counterparts.
617

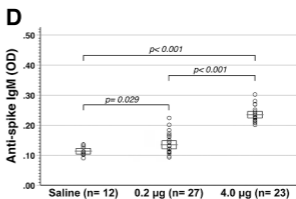
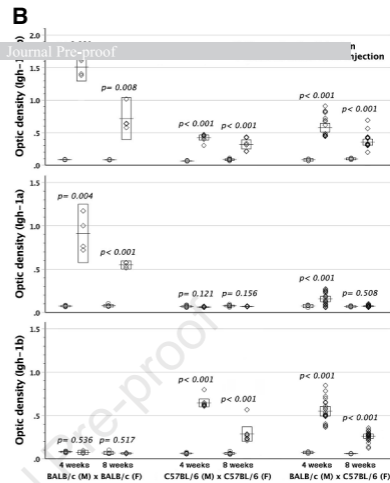
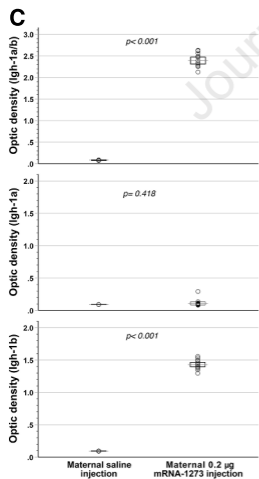
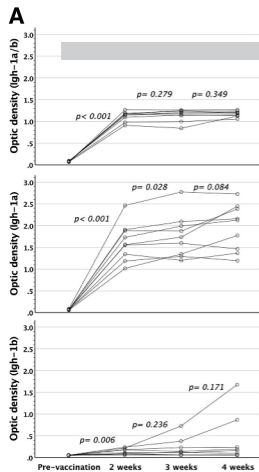
618 **Figure 5. Immunological consequences of in utero mRNA-1273 injection.** GD14 FVB/N
619 fetuses were subjected to intraperitoneal injection of mRNA-1273 (IU mRNA-1273, n= 19).
620 **(A, B)** Postnatally, serum anti-spike IgG₁/IgG_{2a} were examined at the age of 1 month. IU
621 mRNA-1273 led to significantly higher titers of anti-spike IgG₁/IgG_{2a}, as compared with in
622 utero saline injection (IU saline, n= 9). Serum anti-spike IgG₁/IgG_{2a} gradually decreased within
623 postnatal 3 months. Circles interconnected by a line represented IgG₁/IgG_{2a} levels measured at
624 1 (M1), 2 (M2) and 3 (M3) months old from an individual mouse (n= 11). **(C)** Lymphocyte
625 proliferation in response to spike protein was measured by the readout of incorporated tritium
626 (n= 4) as counts per minute (cpm). Medium only was used as background controls, bovine
627 serum albumin (BSA) as third-party stimulators and Con-A as a mitogen to stimulate T-cell
628 population. IU mRNA-1273 significantly proliferated specifically in response to spike protein
629 ($p < 0.027$), whereas IU saline (n= 4) failed to show lymphocyte proliferation under spike
630 protein stimulation. There was a significant difference in lymphocyte proliferation under spike
631 protein stimulation between IU mRNA-1273 and IU saline ($p < 0.006$). Rectangles within a
632 dataset represented 95% confidence intervals for the means, which were shown as transverse
633 lines crossing the rectangles. **(D)** Spike-reactive IFN- γ - and IL-2-secreting cells of splenic
634 lymphocytes was enumerated by Elispot. Figures showed the spots with their counts from the
635 representative mice of IU mRNA-1273 and IU saline. The frequency of spike-reactive IFN- γ -
636 and IL-2-secreting T-cells was calculated by the mean of Elispot readouts (triplicates) divided
637 by the CD3⁺ cell ratio of splenic lymphocytes in each individual mouse.

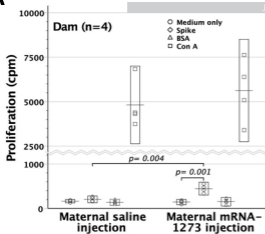
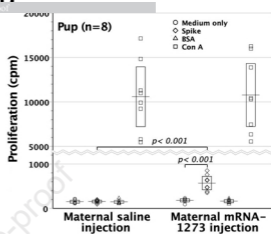
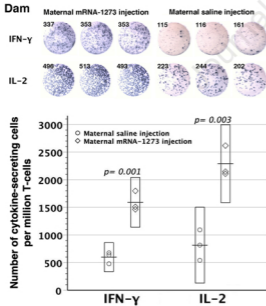
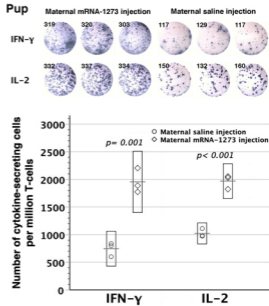
A

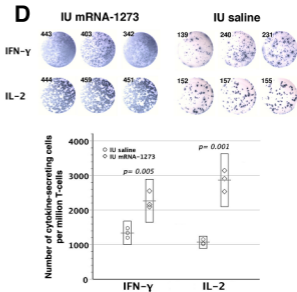
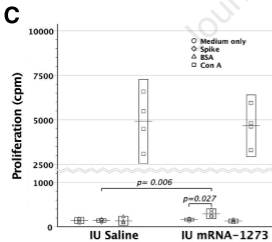
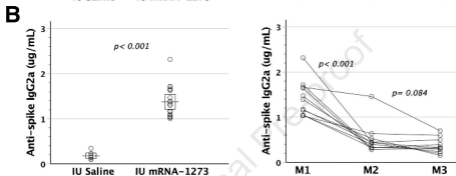
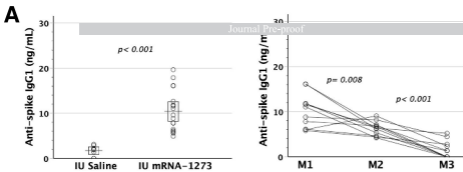
Journal Pre-proof

**B****C****E****D****F**

A**B****C**



A**B****C****D**



Chen and colleagues demonstrated that mRNA-1273 could cross the placenta and show immunogenicity in the fetus following its administration to pregnant mice. It provided the new insight that mRNA vaccine administration to expectant mothers might endow their newborns with not only passive but also active immunity against pathogens.

Journal Pre-proof